Structural Performance of the Second Oldest Glued-Laminated Structure in the United States

Douglas R. Rammer[1], Jorge de Melo Moura[2], and Robert J. Ross[1]

[1]Forest Products Laboratory, US Forest Service, One Gifford Pinchot Drive, Madison WI, 53726, PH (608) 231-9266 drammer@fs.fed.us
[2]Department of Architecture and Urbanization, Universidade Estadual de Londrina, Londrina, Paraná' Brazil jordan@uel.br

ABSTRACT

The second glued-laminated structure built in the United States was constructed at the USDA Forest Products Laboratory (FPL) in 1934 to demonstrate the performance of wooden arch buildings. After 75 years of use the structure was decommissioned in 2010. Shortly after construction, researchers structurally evaluated the glued-laminated arch structure for uniform loading on the center arch. This structural system evaluation was added to the existing laboratory work on glued-laminated arches to develop the foundation on which the current glued-laminated arch design criteria is based. After 75 years of service and decommisioning, recovered arches were tested in the laboratory to evaluate the loss of structural performance. Loss of structural performance was evaluated by comparing original and current deformation. Based on a preliminary visual and structural assessment, the degradation of structural performance was minimal in the arches, except for two arch that were affected by the building fire.

Keywords: Glued-laminated, arch, historical, structural evaluation, ultrasound

INTRODUCTION

In the 1930's the USDA Forest Products Laboratory was engaged in a research program to develop glued-laminated wood beams (Wilson and Cottingham 1952) and arches (Wilson 1939). A seminal project for the glued-laminated research was the construction of the second glued-laminated arch building in the US on FPL's campus in winter of 1934 (Rhude 1996) (Figure 1). This building was 13.7 m wide by 48.8 m long, 5.7m high, and consisted of 9 arch lines spaced 4.8 m apart. Three different arch configurations were utilized. The five central arches were glued-laminated arches with a rectangular cross section having a constant width but a varying depth that was greatest at the knee and least at the foundation and roof peak. On each side of the glued-laminated arches are wooden double "I" section arches composed of plywood webs and glued-laminated flanges with a constant width and varying depth, similar to the glued laminated arches (Figure 1). At either end of the building, heavy timber trusses connected with shear plate connectors span the building width.

Between the arches, stress-skin panels consisting of top and bottom plywood panel, glued and nailed to nominal 38 by 140 mm solid sawn lumber, spaced 1.2m apart, were used.

The arched structure housed various research activities but in 1993 a fire event occurred at the west end of the structure. The resulting damage to building led to the repair of the west end heavy timber truss and double "I" section arches.

After 75 years of use, this structure was deconstructed in the fall of 2010 (Figure 2). Since these glued laminated and double I section arches represent the first generation of both construction adhesives and glued-laminated development, the durability of these arches was mechanically evaluated in a manner similar to the originally 1935 structural loading of the arched building.

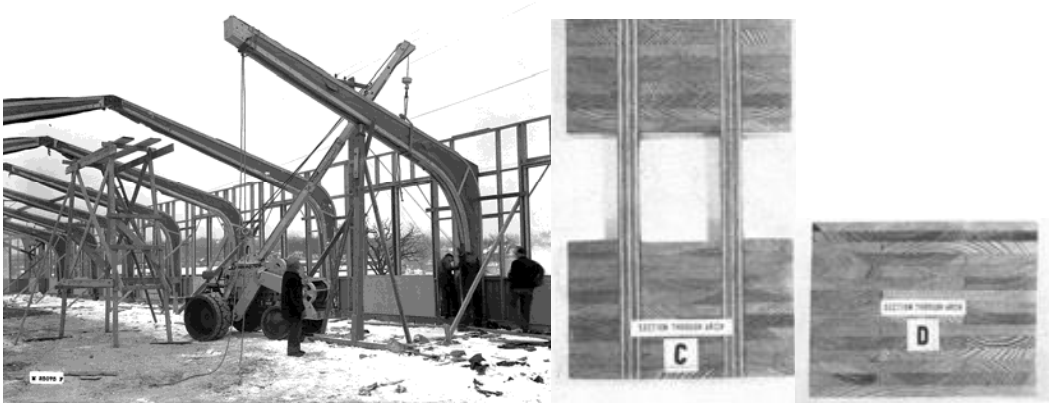

Figure 1—Construction of the arched building in the winter of 1934 using (c) double "I" section and (d) solid glued laminated arches.

Figure 2—Deconstruction of FPL's glued-laminated arch building in 2010.

INITIAL ARCH PERFORMANCE

In the fall of 1935, the glued-laminated arch structure was evaluated by incrementally applying sand bags over the center, full arch until a full 140kN load was achieved (Figure 3). This load is equivalent to a 295 kN/m^2 on the tributary roof area to one arch and 42% higher than the assumed design live load. Both immediate and

sustained deformations were measured from September 1935 to May 1936 (224 days). Deformations were measured on the loaded arch at the peak and quarter points, while only the peak deformations were measured for the two adjacent arches (Figure 3). Based on these measurements, it was determined that the load was distributed to the adjacent arches by the stressed-skin panels (Wilson 1939). Data from this structural evaluation was used to establish both the short term and long-term test procedures used in this study and validated the structural models.

Figure 3— Loading of arch building and measurement techniques for live loading of building.

EXPERIMENTAL PROCEDURES

Tests of a single arch were conducted using a vertical loading configuration and magnitude similar to the original study of the arched structure. To accomplish in the laboratory load distribution affects that occurred in the original structure must be accounted for and a pattern of concentrated loads that approximates a uniform load condition must be determined. This was accomplished through structural analysis of both the original building and a single half arch using MASTAN2 (2006).

To determine the amount of load redistributed away from of the central arch, the entire arched building was modeled and compared to the original measurement data. For the model of the complete building, each arch was sub-divided into 32 beam elements, each with its cross sectional area and moment of inertia equivalent to those of the mid-span element properties. Symmetry was used and the upper and lower arch connections were assumed to be pin type connection. A uniform load, equivalent to the total weight of the sand bags, was applied along the length of the arch arm. The roof system of the arched building consisted of wood stress-skin panels that were attached to the top of the arches with six-penny nails spaced every 140 mm. For modelling, stress skin members were represented as beams spaced every 1.2 m with effective width section properties from Porteous and Kermani (2007). Since the panels were discontinuous over the arch and nails were used to connect the panels to the arch, semi-rigid connections were assumed at the end of the stress-skin beam elements (Figure 4). Effective connection stiffness was adjusted until the model and measured crown deformations of the loaded and adjacent arches along with the ¼ point deformation of the loaded arch matched. Based on the

analysis, instead of applying the original 140kN loading to the single full span arch, the laboratory loading was reduced to 106kN to account for the load distributional effects of the stress-skin roof.

Similarly, a single half arch model was created to determine the number and location of concentrated loads to approximate a uniformly distributed load applied to the arch arm. A linear elastic structural analysis was performed of a single arch that was sub-divided into 52 beam elements with variations in cross sectional properties. An iterative process of locating 4 concentrated load points continued until the difference between the displacements and moments of the different concentrated and uniform loading conditions were visually minimized. Figure 4 shows the arch deformation for both the series of concentrated loads and the uniformly distributed load conditions, which justifies the approach. A similar model was generated for the I-section arches with sectional properties determined assuming fully composite behavior.

The original loading was uniform across the entire width of the building resulting in peak displacements that were only vertical and rotational. Due to the symmetry of the original structure and loading, only half an arched span was loaded in the laboratory. The peak connection was simulated by welding the original connection plates to a stiff plate that ran on a linear bearing system. This linear bearing facilitated the vertical movement of the arch peak and the connection plates allowed for connection rotation similar to the actual building (Figure 5).

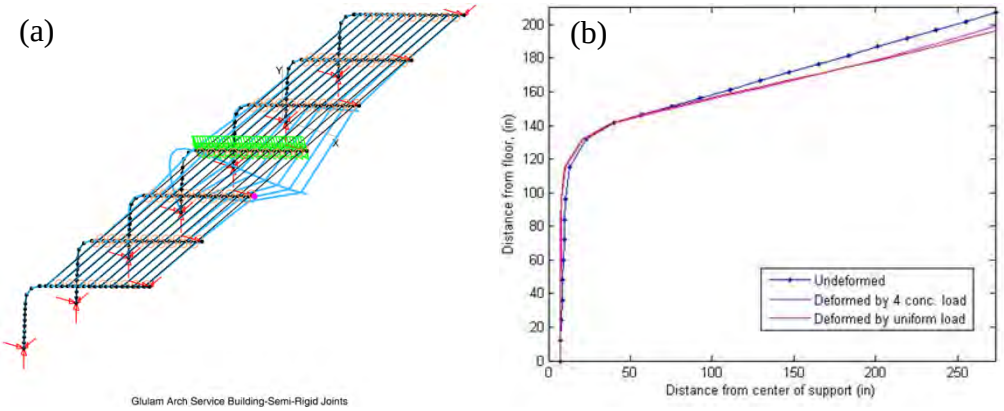

Figure 4—Results of (a)arch building model and (b) comparison of deformations resulting from uniform loading and concentrated loading conditions.

Load was applied to the arch using two 245-kN MTS actuators in tandem under load control until the maximum load of 53kN was reached. This represents half of the original sand bag loading adjusted for distributional effects. Four cycles of load were applied as shown in Table 1 with no pauses at the transitions between cycles. Loading duration in cycle 3 for arches 3 and 10 was extended to 138 and 168 hours, respectively. Figure 6 shows the images of the test setup to achieve the 4-point concentrated load condition. Both load and deformation were continually recorded

for the duration of the tests, at variable rates. Vertical deformations were measured at all quarter points and one horizontal deformation of the arch leg was measured 3.3 m above the support.

Table 1—General Loading Protocol for Arches

Cycle	Loading	Sustained	Unloading
1	5 min	10 min	5 min
2	5 min	10 min	5 min
3	5 min	72+ hours	5 min
4	5 min	10 min	5 min

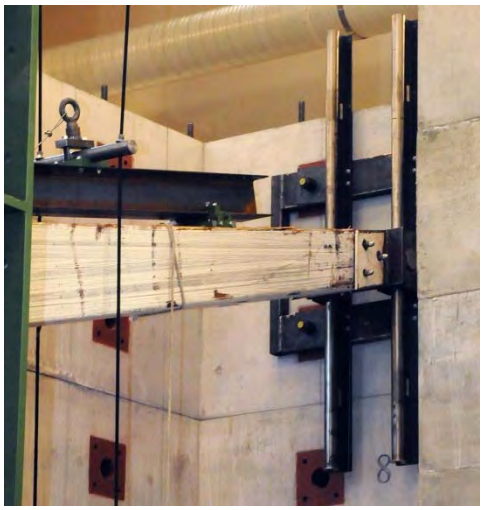

Figure 5—Linear bearing to allow vertical only movement of the crown connection.

Figure 6— Testing setup of one half of single arch with a four-point loading configuration.

EXPERIMENTAL RESPONSE

Short Term Loading- Arches were to be loaded with 2 short-term cycles, followed by a sustained load, and finished with one more cycle of short term loading. Typical responses to the short term loading cycles, readjusted to an initial zero deformation, are shown in Figure 7a. Note the initial cycle had the greatest deformation response due to the seating of the arch while subsequent short term loadings, cycle 2 and cycle 3 showed nearly identical behavior. Only arch 5 showed abnormal behavior and only one short term loading was conducted (Figure 7b). An inspection of the arch 5 revealed the excessive deformation was due to delamination and decay at the base (Figure 8) (Teder and Wang 2013). Due to the location of arch 5 in the building it is believed that delamination and decay were a result of the 1993 fire event. Even though excessive deformation was observed, the arch was loaded to the full load without showing additional signs of distress.

Crown deformation versus applied load, for the third cycle of loading, is plotted in Figure 9 for all arches except 5. Figure 9 shows that all of the arches show a linear response with load, but three distinct observations can be made for the glued laminated arches: 1) arches 1 thru 4 and 7 are grouped together and showed the highest stiffness, 2) arches 8 thru 10 are grouped together at a different and slightly lower stiffness response, and 3) arch 6 stands alone with the lowest linear response. As with arch 5, inspection of the arch 6 base reveled significant delamination along with some signs of charring (Figure 8). A possible explanation for the middle grouping is related to connection integrity, which will be discussed later. Also plotted in Figure 9 is the response of the double "I" section arches. All these arches had stiffer behavior due to the increased cross sectional properties. Repaired double I section arches (13 and 14) were stiffer than the original double "I" section arches indicating the repair was effective but the effectiveness of the repair on stiffness was

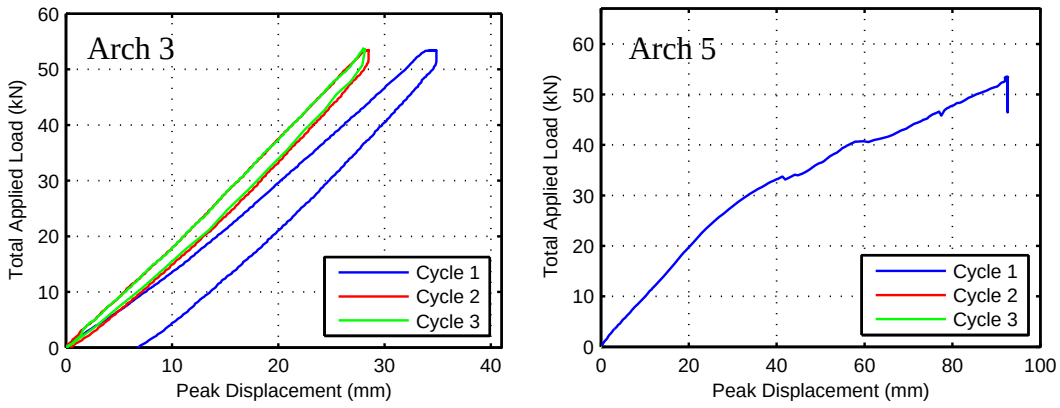

Figure 7— Short term load response for (a) Arch 3 and (b) Arch 5.

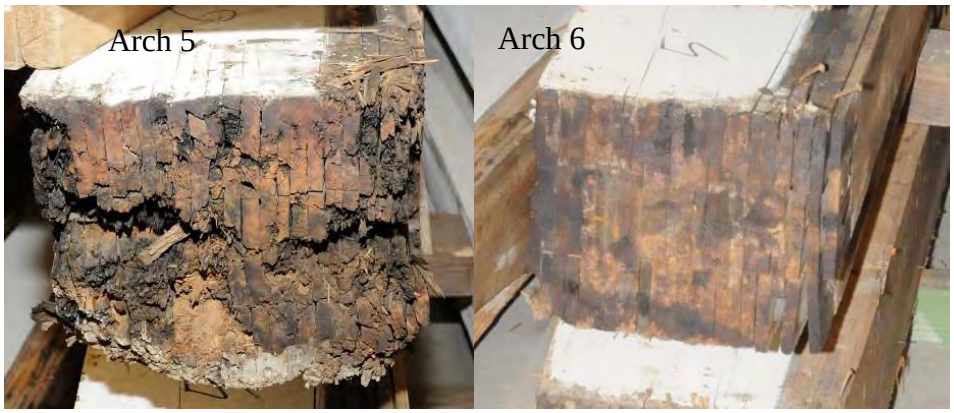

Figure 8— Arch 5 and 6 base end conditions the exhibited significant deterioration from fire event

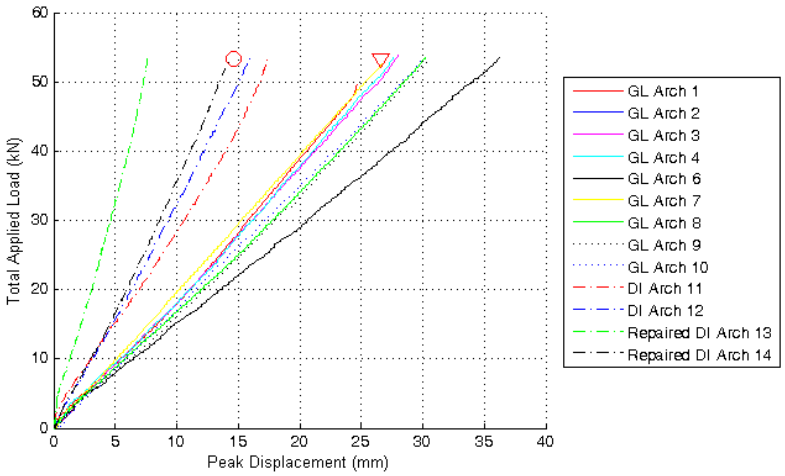

Figure 9— Third cycle, short term load response for all arches (except 5) where ▽ and O are modelled displacement. (GL = Glued Laminated, DI = Double I Section)

significantly different. Arch 13 had significantly more stiffness when compared to arch 14. Based on extent of charring present on arch 14, it is reasonable to assume the fire caused greater damage to this arch, most likely delamination at the glue line. Since the repair was the application of new glued laminated arches to the double "I" section, if one arch has less damage it would result in greater repair stiffness.

Long Duration Loading- A sustained load, maintained for at least 72 hours, was applied to the arches to provide insight into the potential increase for deformation by sustained loading. During the original loading condition, peak deformation increased about 15 to 20 percent after the first 60 days of loading, while the rate of deformation decreased. After 60 days, the original deformation rate increased. This rate change was attributed to member drying associated with the initial heating of the arched building and periodic snow loads that occurred during the winter over the evaluation time. To compare the effect that sustained loading has on deformation for all arches we calculated the ratio of the instantaneous measured deformation to deformation

when maximum load was first applied. Figure 10 plots this deformation ratio versus time (72hours) at all measurement locations for arch 8 and the deformation ratio for the crown measurement for all loaded arches. Larger measured deformations (Peak, ¾ pt, and midspan) gave similar and consistent ratios over the monitoring period. The rate of deformation change was greatest in the first 24 hours of loading and decreased with continued loading. Overall the deformation increased over the entire monitoring period and was independent of arch configuration. For all the arches, the percent of deformation increase was lower than 15 percent and the rate of deformation change was decreasing. These observations lend credence to the statement from Wilson (1939) that measured building deformation changes in the original structure after 60 days were caused by drying of the glued-laminated arches and periodic snow loads, not the original applied loading.

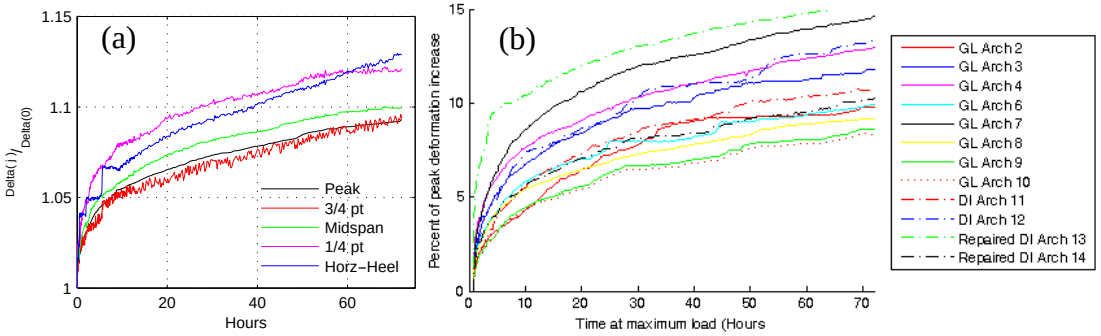

Figure 10— Sustained load deformation response for (a) all measurements for 72 hours and (b) crown deformation for all arches (except 5).

ANALYTICAL RESPONSE

A simple linear elastic model of a single arch was created using MASTAN2, (2006). Though the intention was to simulate uniform loading with four concentrated loads and make a direct comparison, the applied loads were placed at different locations in the laboratory testing. The structural model was reanalyzed for the new loading condition. When the original structure was constructed ASTM D143 bending tests determined the average modulus of elasticity of the laminated arch material was 13.1 GPa. For comparative purposes, the quarter point and thrust deformations at maximum load during the laboratory testing of the arches for the final load cycle will be compared to the model values. Table 2 presents the analytical deformation at the measured deformation locations along with the average, minimum and maximum deformations at maximum load. In general, glued laminated model deformations are lower than the average but greater than the minimum measured deflections. Percent difference of the analytical and measured deformations showed similar trends. Figure 9 shows that the model peak deformation (∇ symbol) and the measure maximum deformation for the stiffest group of arches (1,2,3,4 and 7) are virtually the same.

Table 2—Comparison of Analytical model to experimental measurements for glued lmainated and double "I" arches.

	Deformations (mm)				Percent difference		
Location	Analytical	Average	Min	Max	Average	Min	Max
Glued Laminated Arches[1]							
Peak	26.6	29.3	24.6	36.2	-9.1	8.2	-26.4
¾ Point	20.0	20.1	19.7	27.2	-0.5	1.5	-26.5
½ Point	11.7	13.8	12.4	16.8	-15.0	-5.4	-30.2
¼ Point	3.3	5.1	4.7	6.4	-34.8	-29.2	-48.0
Thrust	-7.5	-6.8	-5.7	-9.3	10.4	31.7	-19.3
I Section Arches[2]							
Peak	14.6	16.6	15.9	17.4	-12.3	-15.9	-8.3
¾ Point	10.6	13.2	12.3	14.1	-19.9	-25.1	-14.1
½ Point	5.9	9.0	8.4	9.6	-34.3	-38.3	-29.6
¼ Point	1.4	3.5	3.3	3.8	-60.3	-62.7	-57.5
Thrust	-4.1	-3.3	-3.5	-3.1	24.2	31.0	18.0
Repaired I Section Arches[2]							
Peak	-	11.1	7.8	14.4	-	-	-
¾ Point	-	9.4	7.6	11.2	-	-	-
½ Point	-	6.6	5.8	7.5	-	-	-
¼ Point	-	2.9	2.7	3.1	-	-	-
Thrust	-	-1.8	-2.6	-1.0	-	-	-

[1]Average represents 9 tests
[2] Average represents 2 tests; therefore maximum and minimum represent each test.

For the two original double "I" section arches the model deformations are lower than observed in the tests. Figure 8 shows that the model double I section crown deformation (O symbol) is to the left of the experimental deformation. While this crown displacement difference is within 20% of the model, the source of the difference is still being sought. As stated previously the repaired double "I" section had varying degrees of effectiveness and Figure 8 shows that the crown peak response for both repairs was greater than unrepaired model predictions.
Table 2 included the maximum deformations for the repaired member to gauge the repair effectiveness relative to the original double "I" section at all measurement locations but no model prediction was created for the repaired condition.

CONNECTION ISSUES

One issue observed after deconstruction of the specifically to the glued-laminated arch structures was the condition of the crown connection. Figure 11 shows the crown connection consisted of steel side plates attached to the each arch arm with three 25.4-mm bolts in a triangular pattern. Measurements revealed inner bolt end spacing was 2.5d, lower than the minimum 4d required by current design standards. As a result, most of the arch had cracks or wood plugs emanating from the inner bolts. Figure 11 also shows missing wood material associated with the lower bolt line though this condition was less common. Unlike the inner bolt, sufficient end

spacing was provided for the outer bolts. There are two possible explanations for damage. One, after the failure of the inner bolts, the remaining capacity of the connection was insufficient to carry a maximum event load that occurred during the service life to the structure. Two, the connection was damage during deconstruction due to possible out of plane twisting of the arch (Figure 2). No damage was observed for the double "I" section arches since the bolt end spacing distances were greater. Arches with the greatest connection damage were also the arches that had the intermediate stiffness behavior that is seen in Figure 9. While the connection had influence on the stiffness of the arch, the effect on ultimate strength in unknown because the cracks did not go completely through the cross section. Under a lateral loading scenario, or as the arches reach maximum loading conditions, the connection condition could have a strong influence on behavior.

Figure 11— Peak connection in building and glued-laminated peak with connection plate removed

CONCLUSIONS

After 75 years of service, ten glued-laminated arches were recovered for structural evaluation from the deconstruction of the second glued-laminated building built in the United States. Arch performance was assessed by comparing the deformations of single half-arches with a structural model. A structural model was developed and validated using data generated from in the original 1939 glued laminated arch study. Laboratory tests of half span arches consisted of three cycles of short-term loading and one long-term loading of at least three days. Comparison of the model and experimental deformation revealed that 8 of the 10 arches performed with little or no stiffness loss. One arch had considerable decay and delamination of its leg, and therefore, loading protocols were not completed. Finally, some failures of the glued-laminated edges at the peak connection were observed and attributed to insufficient end spacing of the bolts that influence the response of the arches. Finally, the double "I" section arches experimental and model behavior were different and repair techniques for the double "I" section arches that were effective but the post fire condition of the original section strong effect the stiffness behavior of the repair.

REFERENCES

Rhude, A. J. (1996). Structural glued laminated timber: History of its origin and early development. Forest Products Journal, Vol. 46(5).

Wilson, T.R.C. (1939). The Glued Laminated Wooden Arch. USDA Technical Bulletin No. 691.

Wilson, T.R.C. and Cottingham, W. S. (1952). Tests of glued-laminated wood beams and columns and development of principles of design. Forest Prod. Lab. Rep. R1687.

MASTAN2 version 3.3, developed by Ronald D. Ziemian and William McGuire, 2006

Teder, M. and Wang, X. (2013). Nondestructive Evaluation of a 75-Year Old Glulam Arch. Proceedings: 18th International Nondestructive Testing and Evaluation of Wood Symposium. General Technical Report FPL-GTR-226. Madison, WI: U.S. Department of Agriculture, Forest Service, Forest Products Laboratory. pg 624:632.

Porteous, J. and Kermani, A. (2007). Structural Timber Design to Eurocode 5. Blackwell Publishing.

In: Proceedings of the Structures Congress 2014, Boston, Massachusetts, April 3-5, 2014. Structural Engineering Institute of ASCE, 2014; pp. 1233-1243.

Structures Congress 2014

PROCEEDINGS OF THE 2014 STRUCTURES CONGRESS

April 3-5, 2014
Boston, Massachusetts

SPONSORED BY
The Structural Engineering Institute (SEI)
of the American Society of Civil Engineers

EDITED BY
Glenn R. Bell, P.E., S.E., F.SEI
Matt A. Card, P.E.

Published by the American Society of Civil Engineers